International Journal of Multimedia and Ubiquitous Engineering
Vol.9, No.3 (2014), pp.145-158
http://dx.doi.org/10.14257/ijmue.2014.9.3.15

An Improved Circuit for Rolling Bearing Fault Detection Based On Square Demodulation and Stochastic Resonance

Zengqiang Ma, Jianhua Liang, Yingna Yang and Yachaona Li

Electrical and Electronics Engineering, Shijiazhuang Tiedao University Shijiazhuang, 050043, China

mzqlunwen@126.com, liangjianhua2015@sina.com, banxiayimeng@163.com, 516059378@qq.com

Abstract

Circuit Research of stochastic resonance (SR) method is a hotspot in the domain of fault detection. Based on the introduction of the original circuit model of double steady-state stochastic resonance, an improved algorithm, which is combining square demodulation and stochastic resonance algorithm, is proposed for rolling bearing fault features extraction in the paper. Before the mixed signals to be analyzed are dealt by SR module, low-frequency signals that contain the rolling bearing fault signal are amplified selectively by the square demodulation module. Then, an improved circuit based on the improved algorithm is designed out with the popular circuit designing software of NI Multisim 10.0. After that, the public general test data from the University of Cincinnati data center bearing (IMS-www.imscenter.net) are used to evaluate the performance of the improved circuit. The experimental results show that the improved circuit not only can be realized easily but also has a higher accuracy in fault features extraction than the original one. What's more, the improved circuit can effectively recognize the typical bearing faults during the whole fault evolution process from weak fault to serious one. Finally, in order to deeply analyze the factors that influencing the fault detection performance of the improved circuit, four parameters, which are the amplitudes and the frequencies of the modulation signal and carrier signal, are selected out and their setting rules are gained based on the corresponding experiments.

Keywords: *improved circuit design, rolling bearing fault detection, square demodulation, stochastic resonance, parameters setting rules*

1. Introduction

Application of stochastic resonance for weak signal enhancement detection is new technologies with a kind of practical application value. 1998, Mitaim proposed the concept of adaptive stochastic resonance [1]. Asdi with others studied the adaptive stochastic resonance and its application in weak signal detection [2]. Hu Gang, Beijing Normal University Professor, had done a lot of work in theory research, which laid the foundation for the further application study of stochastic resonance [3].

In the field of mechanical fault diagnosis, Yonggang Leng, Tianjin University, applied stochastic resonance to the early fault detection of weak characteristic signals [4]. Jiyong Tan, Xi'an Jiaotong University, put forward a novel adaptive frequency shift variable-dimension stochastic resonance algorithm based on a time-frequency index, which can effectively detected high-frequency weak periodic signal from strong noise background [5]. Yuxin Gao,

ISSN: 1975-0080 IJMUE

Tianjin Polytechnic University, designed a parameter adjustment method based on LMS adaptive stochastic resonance cascade algorithm [6]. Dongying Han, Yanshan University, proposed an adaptive band-pass stochastic resonance algorithm based on EMD (empirical mode decomposition) for the detection of multi-frequency signal from background noises [7]. Zengjiang Ma, Shijiazhuang Tiedao University, summarized large parameters regulation rules of stochastic resonance in detail, and used it in rolling bearing fault features extraction [8].

But the accurate value assignment of the SR parameters and their reasonable matching between each other are both difficult problems and selective amplification of the rolling bearing fault signal are uneasy to achieve. Further more, the parameters regulation rules of SR produce little effect for selective amplification of the rolling bearing fault signal from the strong background noise. In order to overcome the above disadvantages of these methods, an improved stochastic resonance circuit with the application of square demodulation before the SR module is proposed in this paper. The experiment results show that the improved circuit not only increases the fault detection ability than the original one but also has several advantages such as simple circuit structure and convenient measuring operation.

2. Rolling Bearing Fault Vibration Model

Rolling bearing can generate two kinds of vibration under the normal operation. One is faulty vibration related to the surface, which reflects the damage condition of the bearing. Natural vibration [9] is another vibration belonging to forced vibration, induced by the crash of rolling element with inner and outer ring. Usually, natural vibration has a large natural frequency at 1~20 KHz, and sometimes up to 80 KHz.

Once some local damage appears in rolling bearing, periodic collision will occurs on contact surface with other components, which is called through vibration (fault vibration). When rolling bearing faults happen, the actual collected vibration signal always contains normal vibration and natural vibration. Various kinds of signals produced by different vibration sources are relatively independent. They are superimposed into the measured vibration signal by way of multiplication or plus, whose multi-mixed mechanism is similar to amplitude modulation. Because the natural vibration signal has the largest amplitude and frequency, the rolling bearing modulation model can be simplified to the formula (1) [10].

$$(1)\quad s(t)=\sum_{j=1}^{m}A_j(1+\sum_{i=1}^{n}r_i\cos(2\pi f_r\cdot i\cdot t+\theta_i))\cos(2\pi f_z\cdot j\cdot t+\phi_j)+n(t)$$

A_j and φ_j are the amplitude and phase of natural vibration of the j order harmonic component; r_i and θ_i are the amplitude and phase of faulty vibration of the i order harmonic component; f_r is the faulty vibration frequency and f_z is the natural frequency; $n(t)$ is the noise signal.

Because $f_z >> f_r$ and $A_j >> r_i$, the faulty signal can be regard as low-frequency weak vibration signal comparing with the high-frequency natural vibration. Therefore, j order harmonic component of the natural vibration can be simplified as follows:

$$(2)\quad x_j(t)=A_j[1+r_1\cos(2\pi f_r t+\theta_1)]\cos(2\pi f_z\cdot j\cdot t+\phi_j)$$

3. Original Circuit for Fault Signal Detection based on SR Algorithm

Because the original circuit for fault signal detection based on SR algorithm is the base for the improved circuit, the SR principle and the original circuit are introduced in this section.

3.1. Principle of SR algorithm

Double steady-state system is the research basis of SR, its structure as shown in Figure 1. The Langevin of formula (3) with double potential wells is typical model to describe nonlinear double steady-state nonlinear system:

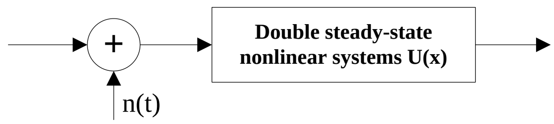

Figure 1. Double steady-state nonlinear stochastic resonance system

$$\frac{dx}{dt} = ax - bx^3 + s(t) + n(t) \tag{3}$$

In the formula (3), x (t) is the system output, s(t) is input signal of the nonlinear systems and n(t) is random noise signal.

3.2. Original circuit based on double steady-state nonlinear SR

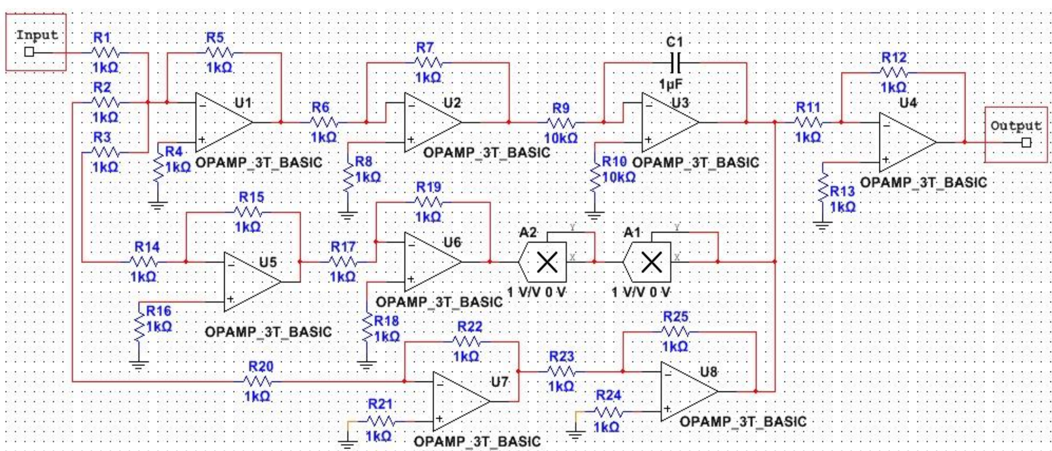

Figure 2. Original circuit based on double steady-state nonlinear SR

As shown in the Figure 2, a circuit, named as original circuit, was designed according to formula (3).

① op amp U7, U8 and resistors R20-R25 constitute the first feedback branch, corresponding to “ax” in the formula (3). Adjustment of parameter a can be realized by changing the resistance of R22 or R25.

② op amp U5, U6, multipliers A1, A2 and resistors R14-R18 constitute the second feedback branch , corresponding to “bx3” in the formula (3). Adjustment of parameter b can be realized by changing the resistance of R15 or R19;

③ op amp U1-U4, capacitor C1 and resistor R1-R13 constitute the backbone circuit. Op amp U1, U2 and resistors R1-R8 constitute a summator that performing accumulation of the input signal, the first feedback signal and the second feedback signal. Op amp U3, capacitor

C1 and resistor R9, R10 constitute an integral circuitry that performing integration of the accumulated signal. op amp U4 and resistors R11-R13 constitute an inverter.

4. The Improved Circuit for Fault Signal Detection

The faulty vibration signal and the natural vibration signal caused by bearing rotation form a kind of AM modulated signal with multi- frequency and high order harmonics. Because the algorithm of square demodulation can enhance low frequency signals, the paper proposes an improved SR algorithm with the square demodulation algorithm is employed to detect weak fault signal. In Figure 3, the part in the dotted line is the improved algorithm proposed in this paper.

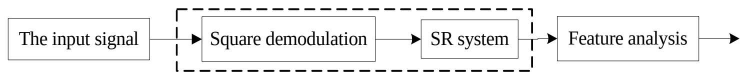

Figure 3. Flow chart of the improved algorithm

4.1. Principle of the improved algorithm

Formula (2) is a simplified function of the natural vibration and it is dealt by square demodulation algorithm as follows:

$$
\begin{aligned}
x_j^2(t) &= A_j^2[1+r_1\cos(2\pi f_r t+\theta_1)]^2\cos^2(2\pi f_z\cdot j\cdot t+\phi_j)\\
&= \frac{A_j^2}{2}[1+\frac{r_1^2}{2}+2r_1\cos(2\pi f_r t+\theta_1)+\frac{r_1^2}{2}\cos(2\pi\cdot 2f_r t+2\theta_1)+\\
&(1+\frac{r_1^2}{2})\cos(2\pi\cdot 2f_z\cdot j\cdot t+2\phi_j)+r_1\cos(2\pi(2f_z\cdot j-f_r)t+2\phi_j-\theta_1)+\\
&r_1\cos(2\pi(2f_z\cdot j+f_r)t+2\phi)+\frac{r_1^2}{4}\cos(2\pi(2f_z\cdot j-2f_r)t+2\phi_j-2\theta_1)+\\
&\frac{r_1^2}{4}\cos(2\pi(2f_z\cdot j+2f_r)t+2\phi_j+2\theta_1)]
\end{aligned} \tag{4}
$$

There are several difference frequency components in Formula (3): DC component, f_r, $2f_r$, $2jf_z$, $2jf_z+f_r$, and $2jf_z\pm 2f_r$. Because $f_z>>f_r$, such frequency components as $2jf_z$, $2jf_z+f_r$, and $2jf_z\pm 2f_r$ are high frequency signals. DC, f_r and $2f_r$ are the low frequency components and their signal amplitudes are $\frac{A_j^2}{2}(1+\frac{r_1^2}{2})$, $A_j^2 r_1$, $\frac{A_j^2}{2}\times\frac{r_1^2}{2}$ respectively. Because $x_j(t)$ in formula (2) is one part of mixed signal to dealt $s(t)$ in formula (1), square processing result of $s(t)$ will also contain DC component, low-frequency fault signal and its low-order harmonic components. Besides, beacause $A_j>>r_i$, the amplitude of the fault signal r_i will be greatly magnified for after multiplication operation and add operation with the amplitude of the natural vibration signal A_j.

4.2. Fault signal detection circuit based on the improved algorithm

Based on the improved algorithm in Section 4.1 and the original SR circuit in Figure 2, the improved circuit is designed as Figure 4 and the square demodulation part is circled by the dotted line.

①V1 is a module designed in LabView and it can transfer the experiment data into the simulation circuit.

②Integrated operational amplifier U9, U10 and resistors R26-R31 constitute attenuator module. Adjusting the value of R26 can avoid waveform distortion caused by signal amplification function of the square demodulation part.

③SR module in Figure 4 is sheet symbol to stand for the original SR circuit in Figure 2.

④XSA1 and XSA2 are the spectrum analyzers to observe input and output signal spectrum.

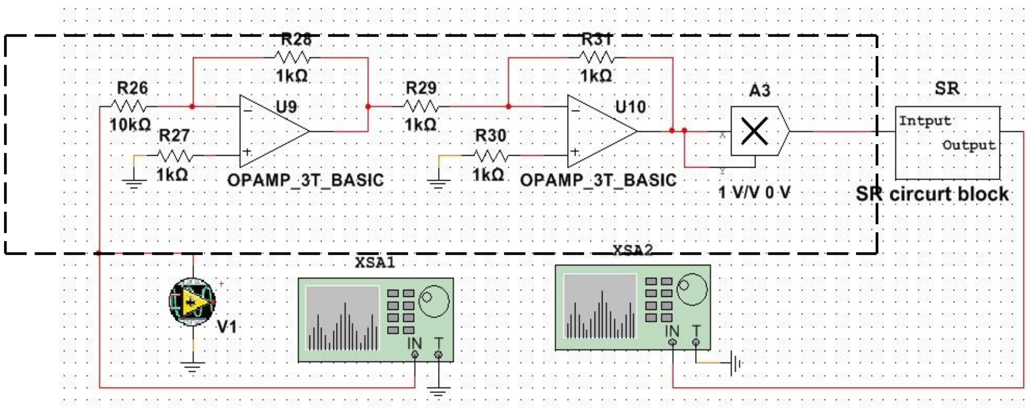

Figure 4. The improved circuit for fault signal detection

4.3. Experiment results comparison between the improved circuit and the original one

4.3.1. Data sources: The data used in the simulation circuit is provided by the University of Cincinnati data center bearing (IMS-www.imscenter.net) in this paper. The entire data packet contains 984 samples collected during six days uninterruptedly and the fault on bearing outer ring appears in the last day. Spectrum analysis is the basic method of rolling bearing vibration diagnosis, so the method is used to extract fault signal in the experiments. Theoretical value of the fault on bearing outer ring, 236.4Hz, is calculated out according to formula (5) based on the bearing parameters showed in Table 1.

Table 1. Bearing parameters in the experiments

Pitch diameter (D/mm)	Roller diameter (d/mm)	Contact angle(α/◦)	Number of rollers (z)	Roller speed (N/r/min)	Sampling frequency (f_s/Hz)	Outer ring fault frequency (f_r/Hz)
71.501	8.407	15.17	16	2000	20K	236.4Hz

$$f_r = \frac{z}{2}(1 - \frac{d}{D}\cos\alpha)\frac{N}{60} \quad (5)$$

4.3.2. Experiment results comparison between the improved circuit and the original one: One data section acquired after the fault on bearing outer ring appeared was used as the input signal for the simulation circuits. Spectrum of the input signal is showed in Figure 5. Spectrum of the output signal from the original circuit is showed in Figure 6 and that from the improved circuit is showed in Figure 7.

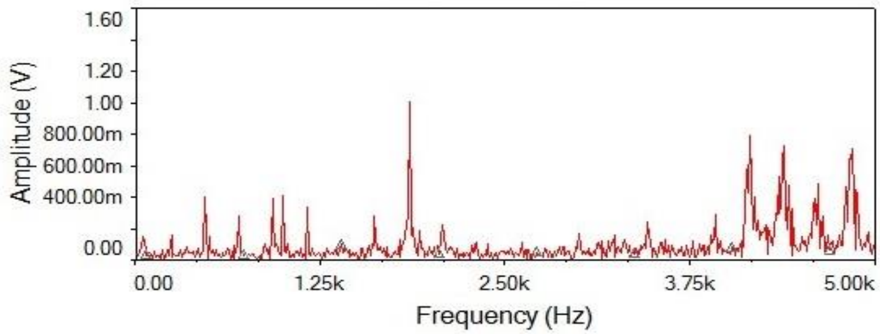

Figure 5. Spectrum of the input signal

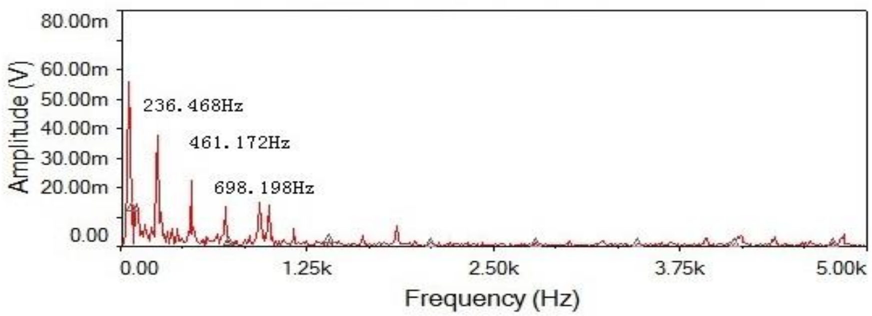

Figure 6. Spectrum of the output signal from the original circuit

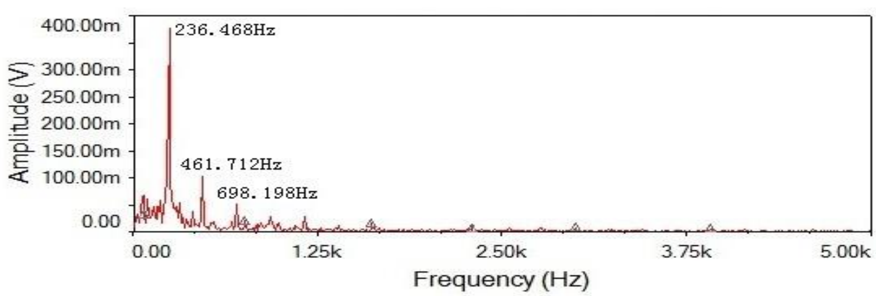

Figure 7. Spectrum of the output signal from the improved circuit

There are three low- frequency components shown in Figure 6 and Figure 7: 236.468Hz, 461.712Hz and 698.198Hz. Because the three spectral components are roughly equal to the one time, two times and three times of the theoretical value of 236.4Hz respectively, they can be regarded as the bearing outer ring faulty frequency, its double frequency and triple frequency. The amplitude comparison of the three spectral components gained by the original circuit and the improved one are given in Table 2. From Figure 5, Figure 6 and Table 2, following conclusions can be drawn:

①There are complex frequency components in the input signal for the circuits and the faulty signal is submerged and difficult to recognize.

②Although the three kinds of faulty components can be discerned from the Fig 5, but there are powerful interference signals in the frequency range less than 234.468Hz and 700Hz ~ 1000Hz.

③Compared with the original circuit, faulty signal detection performance of the improved circuit has been greatly increased.

Table 2. Comparison of the fault signal amplitude gained by the original circuit and the improved one

Frequency component	236.468Hz	461.712Hz	698.198Hz
fault signal amplitude gained by the original circuit(a)	31.820mv	12.782mv	15.207mv
fault signal amplitude gained by the improved circuit(b)	184.613mv	61.882mv	40.188mv
performance improvement percentage: (b-a)/a	480%	384%	163%

4.3.3. Evolutionary process monitoring for bearing fault using the improved circuit: The experiment data from the University of Cincinnati records the entire evolutionary process of the bearing fault, from no fault to fault generation. All of the 984 samples acquired during six days were used as the input signal of the improved circuit and its output signal spectrum shown in Figure 7. From 4:42 am of forth day, the fault feature appeared and increased gradually. According the experiment data From forth day to sixth day, the bearing fault signal amplitude at fundamental frequency, double frequency and triple frequency were recorded and shown in Figure 8, Figure 9 and Figure 10.

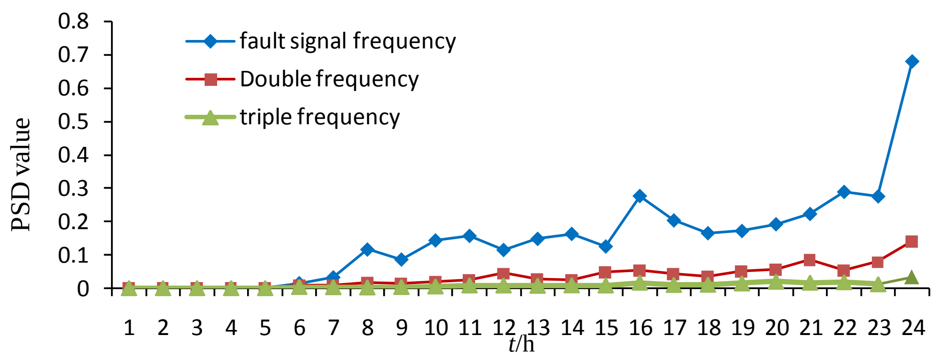

Figure 8. Bearing fault evolution during the forth day

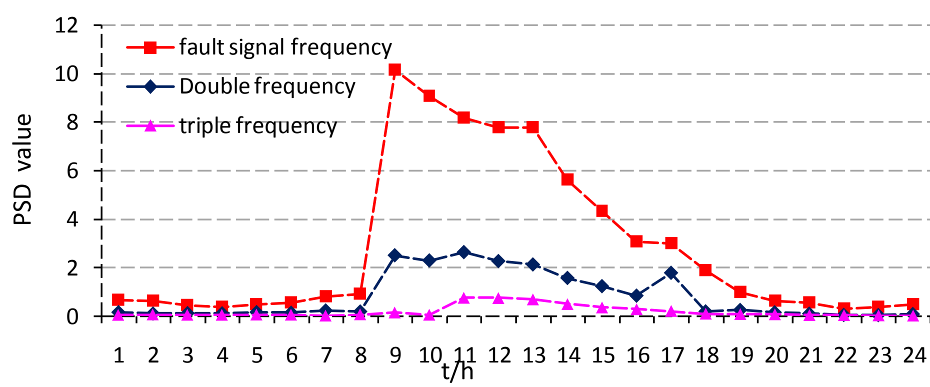

Figure 9. Bearing fault evolution during the fifth day

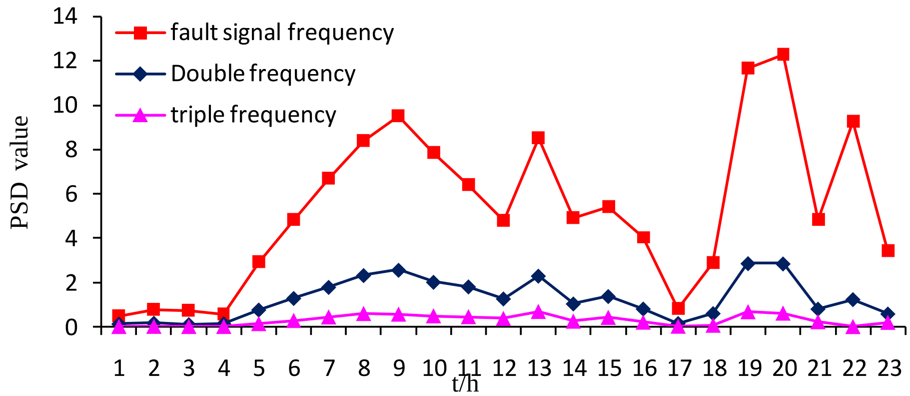

Figure 10. Bearing **fault** evolution during the sixth day

From Figure 8, the fault signal component has not yet appeared during the first four hours. Then, the fault signal component appeared and gradually increased, but maintained a low level. From Figure 9, the fault signal component increased to a high level quickly and this indicated that the bearing outer ring fault became more serious or the surface peeled off. From Figure 10, the fault signal component showed greater fluctuations, and the bearing fault is very dangerous in the actual project.

In conclusion, the bearing fault monitoring results using the improved circuit is identical with the bearing state of Cincinnati, and this means that the improved circuit can monitor the bearing fault effectively.

5. The Impact Factor Analysis for Fault Detection Performance of the Improved Circuit

The analysis in the Section of 4.3 shows that the fault signal detection performance of the improved circuit has been significantly increased than the original one. In order to deeply understand the impact factors for its fault signal detection performance, the mixed signal to be dealt will be decomposed into modulating signal and the carrier signal to investigate how their signal parameters influence the fault signal detection performance of the improved circuit.

5.1. Signal components influencing the fault detection performance of the improved circuit

In order to figure out what kind of signal components influence the fault detection performance of the improved circuit, the rolling bearing fault vibration model that is showed in formula (1) can be simplified as follows: the mixed signal to be dealt will be obtained as formula (6) under the conditions of *m*-1, *n*=1.

(6) $$s_1(t) = A_1(1 + r_1\cos(2\pi f_r t + \theta_1))\cos(2\pi f_z t + \phi_1) + n(t)$$

In formula (6), there are seven uncertain parameters of A_1, r_1, f_r, θ_1, f_z, $\varphi_1$and $n(t)$. Because the initial phase of θ_1 and φ_1 have no effect on the spectrum analysis and the noise $n(t)$ is uncertain, only four parameters of A_1, r_1, f_r and f_z are selected to study how they affect the fault detection performance of the improved circuit in this paper. The four parameters are initialized as A_1=1V, r_1=50mV, f_r =50Hz and f_z =1KHz. The other three parameters are initialized as θ_1=0, φ_1=0 and the SNR (signal noise ratio) = 1000. The AM-modulated signal input to the improved circuit is showed in Figure 11.

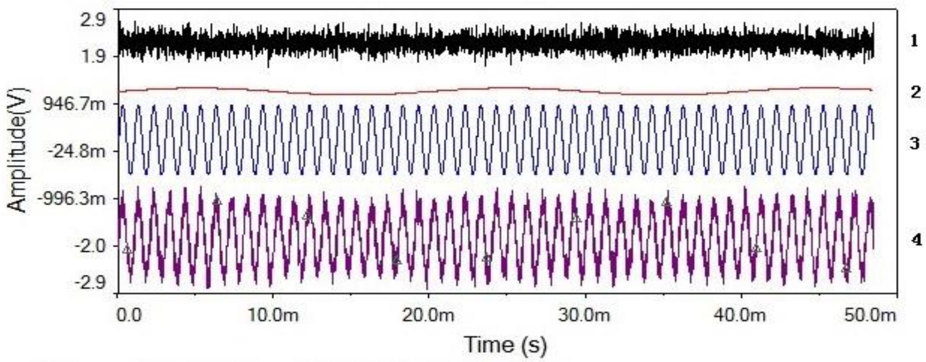

Figure 11. AM-modulated signal components

Curve 1: noise, SNR = 1000;

Curve 2: fault signal using as the modulation signal in the experiment. It can be known that from the Figure 11 that the modulation signal is a weak low-frequency signal;

Curve 3: Carrier signal using as the natural oscillation signal in the experiment. It can be known that from the Figure 11 that its amplitude is stronger and frequency higher comparing with curve 2;

Curve 4: the mixed signal using as the AM-modulated signal input to the improved circuit.

Two spectrums of input signal and the output signal were gained by spectrum analyzer XSA1 and XSA2 (in Figure 4) and shown in Figures 12 and 13 respectively.

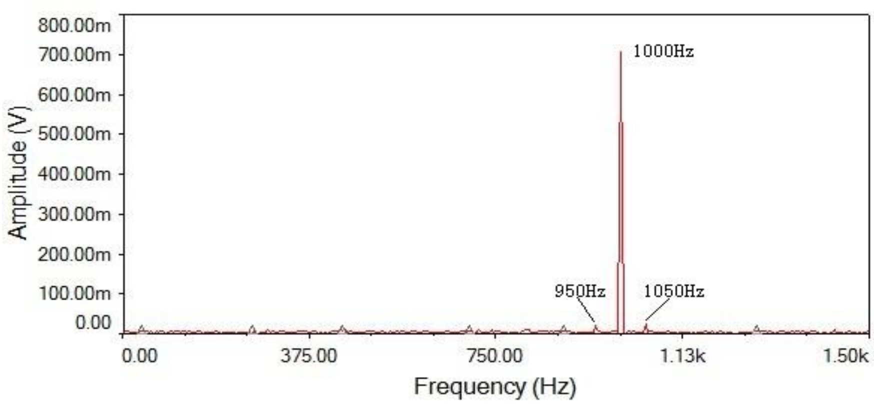

Figure 12. Input signal spectrum of the improved circuit

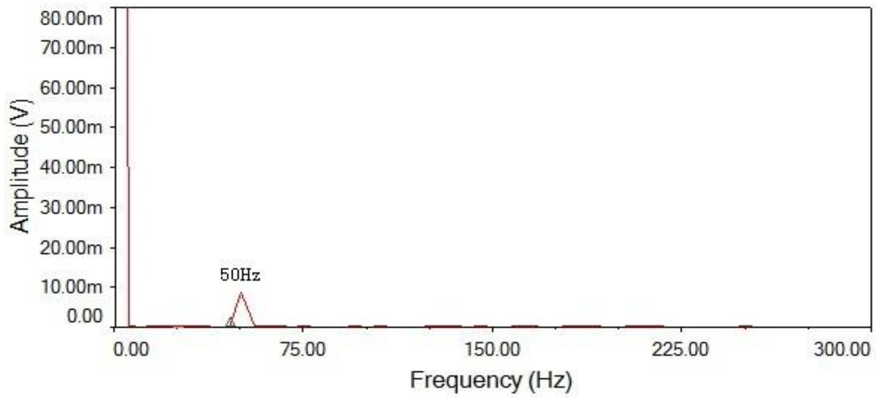

Figure 13. Output signal spectrum of the improved circuit

From Figure 12 and Figure 13, it can be known that the input signal contains the carrier signal of 1000Hz and the output signal contains only the fault signal component of 50Hz. The amplitude of the fault signal extracted by the improved circuit is 100mv, two times the initial value 50mv in the input signal. The experiment result shows that the improved circuit can detect the rolling bearing fault signal accurately.

After the input signal s(t) in formula (6) was transformed by the square demodulation algorithm, its high frequency components can be omitted, recording as s'(t) shown in formula (7), because the latter module of SR has a strong ability of suppressing the high frequency signals.

$$\begin{aligned} s'(t) &= \frac{A_1^2}{2}[1+\frac{r_1^2}{2}+2r_1\cos(2\pi f_r t+\theta_1)+\frac{r_1^2}{2}\cos(4\pi f_r t+2\theta_1)]+n'(t) \\ &= \frac{A_1^2}{2}(1+\frac{r_1^2}{2})+A_1^2 r_1\cos(2\pi f_r t+\theta_1)+\frac{A_1^2 r_1^2}{4}\cos(4\pi f_r t+2\theta_1)+n'(t) \end{aligned} \tag{7}$$

In formula (7), $A_1^2 r_1$ is the output signal amplitude of the improved circuit and it means that only the modulating signal amplitude r_1 and the carrier signal amplitude A_1 have an effect on the fault detection performance of the improved circuit.

Because the low frequency components in s'(t) are the main concern in the fault signal extraction, four parameters of A1, r1, f_r and f_z are selected to study how they affect the fault detection performance of the improved circuit in this paper.

5.2. Influence of modulating signal parameters to the fault detection performance of the improved circuit

In order to figure out how the two fault signal parameters of amplitude r1 and frequency f_r influence the fault detection performance of the improved circuit, the two parameters were taken as f_r =50, 100, 200 Hz, r_1=1, 5, 10, 15, 20, 25, 30, 35 mV and other parameters remained the same in the following experiments. The amplitude of the periodic signal abstracted by the improved circuit is shown in Figure 14 and the corresponding voltage gain of the circuit is shown in Figure 15.

From Figure 14 (a), following conclusions can be drawn:

①In the case of a fixed frequency of the modulating signal, the amplitude of the fault signal increases along with the modulating signal amplitude. It is a linear proportional relationship between the two kinds of amplitudes.

②In the case of a fixed fault signal frequency of f_r, the slope of the fault signal amplitude curve is approximately a constant.

③The slope of the fault signal amplitude curve changes with its frequency, that is, the smaller the frequency, the greater the slope.

From Figure 14 (b), following conclusions can be drawn:

①Voltage gain of the abstracted fault signal is less than 1, although SNR (signal to noise ratio) in the output signal is significantly increased than that in the original input signal. It means that the fault signal decays more significantly and the noise signals at the same time.

②the slope of the fault signal voltage gain curve is close to zero. It indicates that the fault signal voltage gain is not affected by the amplitude but the frequency of the modulating signal. Further more, the smaller the frequency, the greater the slope.

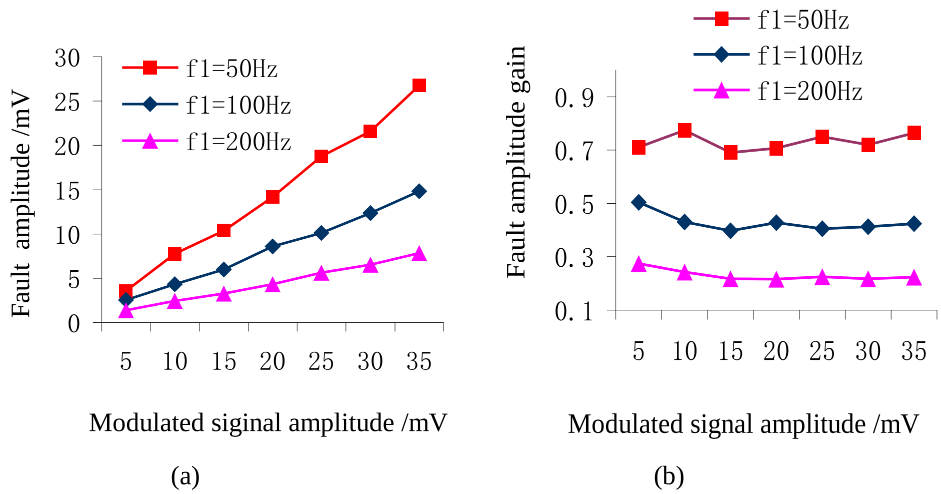

Figure 14. Curves of fault signal voltage amplitude and its gain varying with modulating signal amplitude

5.3. Influence of carrier signal parameters to the fault detection performance of the improved circuit

Under the condition of a = 1, b = 1 (SR structure parameters), the output signal of the improved circuit were recorded as two carrier signal parameters of A_1 and f_z Changing their values. Figure 15 (a) and Figure 15 (b) show how the carrier signal amplitude A_1 influences the fault signal amplitude and the fault signal gain respectively. Figure 16 (a) and Figure 16 (b) show how the carrier signal frequency f_z influences the fault signal amplitude and the fault signal gain respectively.

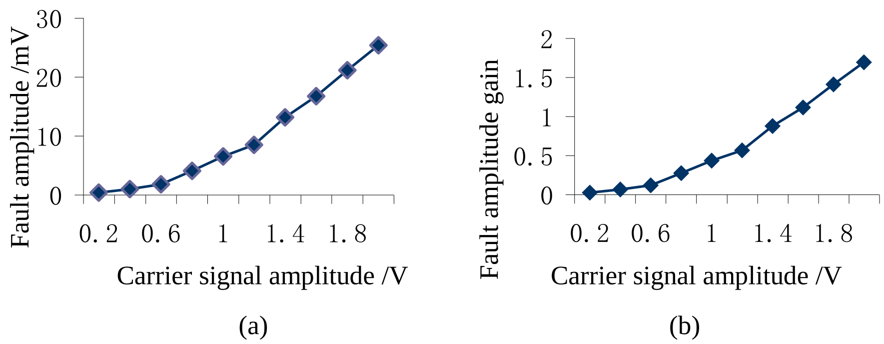

Figure 15. Influence of the carrier signal amplitude to fault signal amplitude and its gain

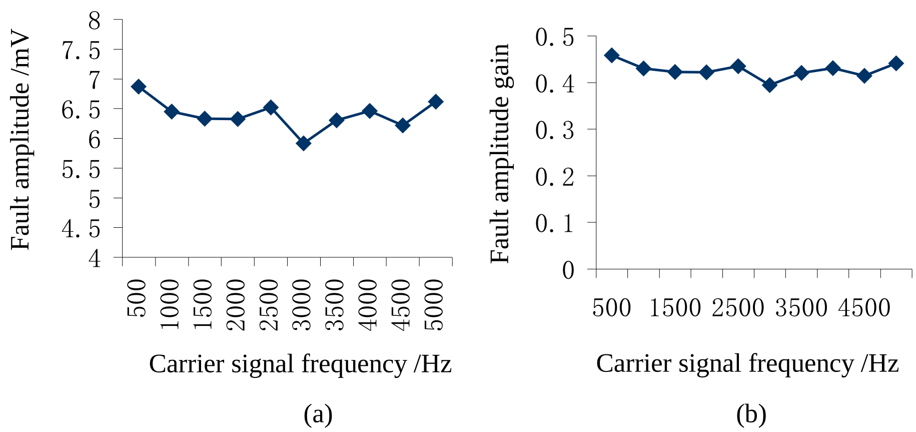

Figure 16. Influence of the carrier signal frequency to fault signal amplitude and gain

① The cures in Figure 15 (a) and Figure 15 (b) look like parabola lines. It means that the fault signal amplitude and its gain are all proportional to the square of the carrier signal amplitude A_1;

②The cures in Figure 16 (a) and Figure 16 (b) look like horizontal lines. It means that the fault signal amplitude and its gain are not changing with the carrier signal frequency f_z, in other words they are not influenced by f_z.

6. Summary

Based on the simplified model of rolling bearing fault vibration modulation, an improved method combined with the square demodulation algorithm and SR algorithm is proposed and corresponding circuit is designed in the paper. In order to test the fault detecting performance of the improved circuit, the bearing vibration monitoring data from the University of Cincinnati rolling data centers was used as the input signal. Experimental results show: the improved circuit structure not only has a higher performance to detect rolling bearing faults than the original circuit but also can be able to efficiently monitoring the evolution process of the rolling bearing fault from weak fault to serious one.

In order to deeply analyze the factors that influencing the functional features of the improved circuit, four parameters of the input signal, which are the amplitudes and the frequencies of the modulation signal and carrier signal, are selected out through the theoretical analysis. Finally, the rules that how the four parameters influence the fault detection performance of the improved circuit were figured out through the corresponding experiments.These rules can provide valuable theoretical basis for using the improved circuit in wider application fields except for the rolling bearing fault detection.

Acknowledgements

This research is supported by National Natural Science Funds of China Key Program (11227201), National Natural Science Foundation of China (11372199, 11202141).

References

[1] Q. Li, T. Wang, Y. Leng and Y. -g. Xu, "Weak Signal Detection Based on Step-Changed Stochastic Resonance", Journal of Tianjin University, no. 4, **(2006),** pp. 432-437.
[2] J. Tan and X. Chen, "Adaptive Frequency-Shifted and Re-Scaling Stochastic Resonance with Applications to Fault Diagnosis", Journal of Xi'an Jiaotong University, vol. 43, no. 7, **(2009),** pp. 69-73.
[3] Y. Gao and F. Wang, "Adaptive cascaded-bistable stochastic resonance system research and design", Journal of Computational and Theoretical Nanoscience, vol. 10, no. 2, **(2013),** pp. 318-322.
[4] D. Han, X. Ding and P. Shi, "Multi-frequency weak signal detection based on EMD after de-noising by adaptive re-scaling frequency-shifted band-pass stochastic resonance", Journal of Mechanical Engineering, vol. 49, no. 8, **(2013),** pp. 10-18.
[5] Z. Ma, Y. Yang and S. Zhong, "Rolling bearing failure feature extraction based on large parameters stochaitic resonance", Journal of Computational Information Systems, vol. 9, no. 16, **(2013),** pp. 6643-6650.
[6] X. Li, A. Zheng and X. Zhang, "Rolling element bearing fault detection using support vector machine with improved ant colony optimization", Measurement, vol. 46, no. 8, **(2013),** pp. 2726-2734.
[7] G. Hu, "Nonlinear systems with random force", Shanghai Science and Technology Education Press, **(1992),** pp. 222-223.
[8] S. Mitaim and B. Kosko, "Adaptive stochastic resonance", Proc. of the 1998 IEEE, vol. 86, no. 11, (**1998**), pp. 2152-2183.
[9] A. S. Asdi and A. H. Tewfik, "Detection of weak signals using adaptive stochastic resonance", Proceeding of the 1995 IEEE International Conference on Acoustics, Speech, and Signal Processing, **(1995)**, pp. 1332-1335.
[10] Z. Wang, "Constraint independent component analysis and the application in rolling bearing fault diagnosis", D: Shanghai Jiaotong University, **(2011).**

Authors

Zengqiang Ma

Borned in Hebei province of China, 1975. Ph.D. degree was earned in major of vehicle engineering, Beijing Jiaotong University in 2011. Major Field of study is digital signal processing. He has published many papers in recent years and more than ten of them were included in the international Engineering Index (EI). Current and previous research interests include signal processing and network measurement & control system.

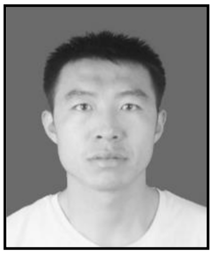

Jianhua Liang

He received his Bachelor in Electrical Engineering and Automation (2012) and postgraduate in Shijiazhuang Tiedao University. His current research interests include different aspects of Signal Processing.

Yingna Yang

She received her Bachelor in in Science and Technology of Electronic Information (2012) and postgraduate in Shijiazhuang Tiedao University. Her current research interests include different aspects of Signal Processing.

Yachao Li

He received his Bachelor degree in Science and Technology of Electronic Information (2013) and postgraduate in Shijiazhuang Tiedao University. His current research interests include different aspects of Signal Processing.